



## City Research Online

### City, University of London Institutional Repository

---

**Citation:** Njoum, H. & Kyriacou, P. A. (2017). Photoplethysmography for an independent measure of pulsatile pressure under controlled flow conditions. *Physiological Measurement*, 38(2), pp. 87-100. doi: 10.1088/1361-6579/38/2/87

This is the accepted version of the paper.

This version of the publication may differ from the final published version.

---

**Permanent repository link:** <https://openaccess.city.ac.uk/id/eprint/16171/>

**Link to published version:** <https://doi.org/10.1088/1361-6579/38/2/87>

**Copyright:** City Research Online aims to make research outputs of City, University of London available to a wider audience. Copyright and Moral Rights remain with the author(s) and/or copyright holders. URLs from City Research Online may be freely distributed and linked to.

**Reuse:** Copies of full items can be used for personal research or study, educational, or not-for-profit purposes without prior permission or charge. Provided that the authors, title and full bibliographic details are credited, a hyperlink and/or URL is given for the original metadata page and the content is not changed in any way.

---

---

---

City Research Online:

<http://openaccess.city.ac.uk/>

[publications@city.ac.uk](mailto:publications@city.ac.uk)

---

# Photoplethysmography for an independent measure of pulsatile pressure under controlled flow conditions

Haneen Njoum and Panayiotis A Kyriacou

Research Centre for Biomedical Engineering, City University London, London, EC1V 0HB, UK

E-mail: [haneen.njoum.1@city.ac.uk](mailto:haneen.njoum.1@city.ac.uk)

## Abstract

Noninvasive continuous blood pressure measurements are desirable for patients and clinicians. This work proposes and validates a method for transmural pressure measurement using photoplethysmography (PPG) in an *in vitro* setup that allows control of pressure and flow conditions. The optimum pulsatile volume measure is obtained by comparing parameters extracted from the photoplethysmographic signal (AC amplitude, normalized pulse volume (NPV) and adjusted pulse volume (APV)). Pulsatile volume can then provide pressure measurements using the exponential pressure–volume ( $P$ – $V$ ) relationship and validated using the gold standard catheter pressure measurement. Pressure, red (R) and infrared (IR) PPG signals were recorded continuously in two arterial models with different cross-sectional areas (Model 1 and Model 2) utilising a pulsatile pump. Flow rates were controlled by varying pumping frequencies at low and high stroke volumes. The optimum method for estimation of the pulsatile volume is through APV, which had a highly significant correlation ( $r^2 = 0.99$ ,  $p < 0.001$ ) for Model 1 and ( $r^2 = 0.98$ ,  $p < 0.001$ ) for Model 2. APV obtained a significantly better fit when compared to  $NPV_{IR}$  ( $r^2 = 0.73$ ,  $z = 25.85$ ,  $p < 0.001$ ),  $NPV_R$  ( $r^2 = 0.95$ ,  $z = 12.26$ ,  $p < 0.001$ ),  $IR_{AC}$  ( $r^2 = 0.52$ ,  $z = 28.29$ ,  $p < 0.0001$ ) and  $R_{AC}$  ( $r^2 = 0.92$ ,  $z = 15.27$ ,  $p < 0.0001$ ) in Model 1, and when compared to  $NPV_{IR}$  ( $r^2 = 0.92$ ,  $z = 10.23$ ,  $p < 0.0001$ ),  $NPV_R$  ( $r^2 = 0.96$ ,  $z = 5.08$ ,  $p < 0.001$ ),  $IR_{AC}$  ( $r^2 = 0.63$ ,  $z = 22.47$ ,  $p < 0.0001$ ) and  $R_{AC}$  ( $r^2 = 0.92$ ,  $z = 17.70$ ,  $p < 0.0001$ ) in Model 2. These preliminary findings suggest that APV could be used as a potential non-invasive continuous method of blood pressure measurement at different flow conditions.

Keywords: photoplethysmography, non-invasive pressure, hemodynamics, diagnostics, optical sensors, blood pressure

(Some figures may appear in colour only in the online journal)

## 1. Introduction

Hypertension is the most common condition seen in primary care and is known to lead to myocardial infarction, stroke, renal failure, and death if not detected early and treated appropriately (James *et al* 2014). A large body of evidence, from randomised controlled trials, has shown the benefits of antihypertensive drug treatments in reducing important health outcomes in hypertensive patients (Staessen *et al* 1997, Beckett *et al* 2008). Nevertheless, there is also evidence that specific drug classes may differ in some effect or in special groups of patients (National High Blood Pressure Education Program 2004, Members *et al* 2013). Noninvasive continuous blood pressure (BP) measurement could be proven to be a suitable tool to assess the effectiveness of pharmacological and also non-pharmacological treatments.

Noninvasive measurement of blood pressure using the auscultatory method provides adequate data for many applications in medicine. However, some limitations are present that challenge their applicability in certain clinical situations such as; (1) the method can only provide intermittent measurements, a pause of 1–2 min between two BP measurements is necessary to avoid errors (Campbell *et al* 1990), therefore, short-term changes in BP cannot be detected; (2) the inflation of the cuff may disturb the patient and as a consequence, alterations of the BP can be observed; (3) errors in the technique of the measurement might arise due to the conditions of measurement and arm position. Such problems are more relevant when investigating BP fluctuations in critically ill patients, infants or during sleep. An alternative approach is continuous, noninvasive measurement of BP which is desirable for monitoring patients during and after a major surgical operation or in intensive care units and for home health care. Photoplethysmography (PPG) is one of the methods utilised for this purpose using the vascular unloading method and pulse wave velocity (PWV) approach.

The vascular unloading technique uses Infrared (IR) transmission PPG to provide ‘raw’ continuous pressure readings in commercial devices such as the Finapres, the CNAP, and Nexfin (Gibbs *et al* 1991, Stokes *et al* 1991, Jeleazcov *et al* 2010, Weiss *et al* 2014). In these technologies, Finger-IR PPG detects changes in blood volume and is used in conjunction with a finger cuff and a servo-controlled pump which adjusts cuff pressure to maintain a constant finger blood volume. However, the technique is less accurate during hypotension events or at alternating vascular tone (Ilies *et al* 2012). Other limitations include the potential for patient discomfort due to the need for repeated calibration with the brachial artery pressure using an oscillometric cuff. The technique is also known to incur reduced precision during periods of hemodynamic instability which makes it an unsuitable alternative to direct pressure monitoring (Weiss *et al* 2014). Moreover, the available commercial devices come with a high price tag and are not well suited for personal or home use. Pulse wave velocity (PWV) is the speed of a pressure pulse propagating along the arterial wall and can be calculated from pulse transit time (PTT). This method has been investigated using a combination of ECG and PPG signals (Foo and Lim 2006). While few studies consider the method to be reliable (Ahlstrom *et al* 2005, Gesche *et al* 2012), some question the reliability of this approach as a clinical device (Young *et al* 1995, Payne *et al* 2006). Investigation in a large number of subjects showed that age, BP, gender and cardiovascular risk factors significantly influence PWV (Yamashina *et al* 2002, Foo and Lim 2006). The studies suggest that PWV can only be used for measurement

of relative BP changes and may encounter errors due to the effect of BP on the measurement and the variability of arterial elasticity from one individual to another or due to neurohormonal factors.

To investigate the potential of PPG as a technique for noninvasive pressure measurements, a more fundamental approach to PPG analysis is proposed. PPG is an optical technique mainly applied in pulse oximetry for estimating blood oxygen saturation. The sensor commonly uses red (R) and infrared (IR) light sources and a photodetector and is attached to a skin surface. The signal provides an oscillatory component ( $PPG_{AC}$ ) and another steady component ( $PPG_{DC}$ ). Despite the simplicity of the technique, the origin of both components is not well understood (de Trafford and Lafferty 1984, Jespersen and Pedersen 1986, Shelley 2007). The latter is believed to generate from the low frequency varying functions, such as respiratory and thermoregulation and the former is assumed to reflect blood volume change (Kyriacou 2013, Abay and Kyriacou 2015). What both components denote hemodynamically have not been clarified in a strict manner. A quantification method is constrained by both measures due to the gain-dependant nature of the signal. Possibly due to such limitations the raw PPG components have been obtained less frequently than other parameters such as blood pressure or heart rate (Nijboer *et al* 1981, Allen 2007).

Few studies explored the potential of the amplitude of the  $PPG_{AC}$  in providing a direct measurement of blood pressure. It was reported that the magnitude of the  $PPG_{AC}$  is considerably more reliable in providing a measure of arterial blood pressure when compared to PWV. However, such findings encountered inaccuracies in standing positions when compared to supine positions or weakened correlations during REM sleep phases (Chua and Heneghan 2006, Chua *et al* 2010).

The aim of this paper is to present an alternative strategy for the direct measurement of noninvasive pressure measurements using the PPG components to overcome the previously discussed limitations. This study presents an investigation of the relationship between the PPG and pressure signals in an *in vitro* setup, assuming an exponential pressure–volume ( $P$ – $V$ ) relationship. PPG components at distinct wavelengths were investigated at varied flow rates, following changes in the pumping frequency and stroke volume of a pulsatile pump in models of a large and small artery. normalised pulse volume (NPV) is advocated on the basis of the optical model in the human circulation expressed by Beer–Lambert’s law at each wavelength. Similarly, adjusted pulse volume (APV) is defined on the basis of Beer–Lambert’s law utilising both wavelengths considering the different penetration depths of each wavelength (Ilies *et al* 2012). This is performed in an effort to consider the effect of the oscillatory and the steady components of the pulsatile flow, as commonly known from a fluid dynamics point of view (Stokes *et al* 1991).

### 1.1. Principle

$P$ – $V$  relationship is known to follow an exponential behaviour in the human circulation (Baker *et al* 1997, Burkhoff *et al* 2005) as noted in (1). Our assumption is that this practice is valid in the developed *in vitro* model which mimics the mechanics of the human circulation.

$$P = b \exp(nV) \quad (1)$$

Here  $b$  and  $n$  are parameters of the model.

When we record PPGs from an arterial model, total light intensity can be written as a function of fluid volume, given that the distance between the light sources and the photodetector is constant. The pulsatile volume is a combination of an oscillatory component ( $\tilde{V}_0$ ) and a steady

component ( $\tilde{V}_s$ ). Assuming that the Beer–Lambert law holds, the following equation expresses the relation between the total incident ( $I_0$ ) and total transmitted light ( $I$ ):

$$I = \exp(-\varepsilon_s c_s \bar{V}_s) \exp(-\varepsilon_o c_o V_o) I_0 \quad (2)$$

Where,  $c$  is the concentration of the light-absorbing substance in each component and  $\varepsilon$  is the absorbance coefficient. The subscripts, o and s, denote oscillatory and steady components respectively. Given that ( $\bar{V}_s$ ) is constant at the same pressure and wall elasticity, the following equation holds for the steady volume component:

$$\bar{I} = \exp(-\varepsilon_s c_s \bar{V}_s) I_0 \quad (3)$$

Where, ( $\bar{I}$ ) is constant light intensity obtained from the steady volume layer.

Hence, from (2) and (3), the following can be derived

$$\tilde{V}_o = (-\varepsilon_o c_o)^{-1} \cdot \ln(\Delta I_{\lambda_1} / \bar{I}_{\lambda_1}) \quad (4)$$

Where  $\Delta I_{\lambda_1}$  is the amplitude of the oscillatory optical signal, and  $\bar{I}_{\lambda_1}$  is the level of the steady optical signal, at a particular wavelength  $\lambda_1$ . It is noted that  $\ln(I_{\lambda_1} / \bar{I}_{\lambda_1})$  is in direct proportion to the oscillatory component of the total fluid volume ( $\tilde{V}_o$ ), via the unknown constant term ( $\varepsilon_o c_o$ ), presuming that both are constant. Hereafter, normalized pulse volume (NPV) is given by:

$$\text{NPV} = -\ln(\Delta I_{\lambda_1} / \bar{I}_{\lambda_1}) \quad (5)$$

The reliance of the penetration depth on light wavelength is well documented (Stolik *et al* 2000), and this concept is used in deriving the adjusted pulse volume (APV). The volume of steady flow layer is known to develop in the centre of the tube, where light with higher wavelength provides a better estimation, and the oscillatory flow occurs in layers closer to the wall, where shorter wavelengths provide a more accurate estimate, therefore:

$$\bar{I}_{\lambda_2} = \exp(-\varepsilon_o c_s \bar{V}_s) I_0 \quad (6)$$

Given that  $\lambda_2 > \lambda_1$ , (2) and (6) lead to

$$\tilde{V}_o = (-\varepsilon_o c_o)^{-1} \cdot \ln(\Delta I_{\lambda_1} / \bar{I}_{\lambda_2}) \quad (7)$$

Given that ( $\varepsilon_o c_o$ ) is constant. Hereafter, the adjusted pulse volume (APV) is referred to as

$$\text{APV} = -\ln(\Delta I_R / \bar{I}_{IR}) \quad (8)$$

Equation (1) can be logarithmically transformed to be rewritten as:

$$\ln(P_s) = nV_o + \ln(b) \quad (9)$$

Where,  $P_s$  is the systolic pressure signal that drives the oscillatory fluid volume. It was previously noted that NPV and APV are in direct proportion to the oscillatory component of the fluid volume ( $\tilde{V}_o$ ) via the unknown constant term ( $\varepsilon_o c_o$ ). In this study, both parameters are kept constant in a controlled setup to validate the derived relationship. Therefore, (9) can be finally rewritten to give the following:

$$\ln(P_s) = -n \cdot \text{NPV}_R + \ln(b) \quad (10)$$

$$\ln(P_s) = -n \cdot \text{NPV}_{IR} + \ln(b) \quad (11)$$

$$\ln(P_s) = -n \cdot \text{APV} + \ln(b) \quad (12)$$

## 2. Materials and methods

An *in vitro* study was carried out to determine the optical response of PPG<sub>AC</sub> and PPG<sub>DC</sub> of R and IR signals at different flow rates. The *in vitro* setup, described in the following subsections was designed to simulate the flow conditions observed in the healthy and diseased human circulation in the range of 45–180 mmHg mean pressure values.

### 2.1. *In vitro* prototype

A pulsatile flow loop illustrated in figure 1 was designed and fabricated to contain an elastic tube model that produces a range of patterns of mechanical forces at the inner surface of the flexible tubing. A pulsatile pump (1423 PBP, Harvard Apparatus, US) was used to generate the pulsatile flow. The pump permitted flow regulation by two means: (1) controlling the stroke volume, (2) and the pumping rate. A custom-made Plexiglas fluid reservoir (volume: 8 l) contained the fluid within the circulation, was also constructed.

A flexible polyvinyl chloride (PVC) tubing (length: 20 cm, outside diameter (OD): 22 mm, and an inner diameter (ID): 16 mm) was connected to the input of the system to enable a fully developed flow before entering the model. The model consisted of a PVC tube (Model 1) which simulates a large artery and a Tygon tube (Model 2) which simulates a small artery. The mechanical properties of each model are listed in table 1.

The model was mounted onto a specially designed support system which incorporated rubber clamps to hold the tubes at a constant length without interfering with their movement. An initial axial stretch of 1–2% was used to ensure that the flexible tubes remained in a straight position during the pumping phase. One-way check valves with preset opening pressure (50 mmHg) were introduced at both ends of the model which provided the control over the resistance and reflected flow. Valves were also added at the entrance of the design to allow control of flow paths and switch to the bypassing tube to eliminate any bubbles in the system. The room temperature during all *in vitro* experiments was maintained at  $23 \pm 0.5$  °C.

### 2.2. Sensors and instrumentation

**2.2.1. Sensors.** The reflectance photoplethysmography sensor used was designed and fabricated. Two LEDs, R and IR, at a peak wavelength of 640 nm and 860 nm respectively, were aligned in a reflectance mode at a three mm distance from the photodiode (PD) (Vishay, UK). A 3D printed (Makerbot, US) encasing was designed and produced to fix the probe at one mm contact gap with the pulsating tube without interfering with its motion. The pressure was measured at the entrance of the model using a catheter-tip transducer (Harvard Apparatus, US) inserted through the lumen of the model. Flow rate was measured at the centre of each tube using the MD2 ultrasound Doppler (Huntleigh Healthcare, UK) with an 8 MHz probe. A 3D printed holder was designed to fix the probe at a 60° angle with the tube without interfering with the wall motion.

**2.2.2. Optical processing system.** For the acquisition of PPG signals, a custom-made two-channel dual wavelength PPG instrumentation system was designed. The PPG processing system was constructed on printed circuit boards to pre-process and convert the detected current into voltages for later acquisition. The processing system used multiplexed current sources (set to 25 mA) to drive both red and infrared LEDs consecutively. The microcontroller

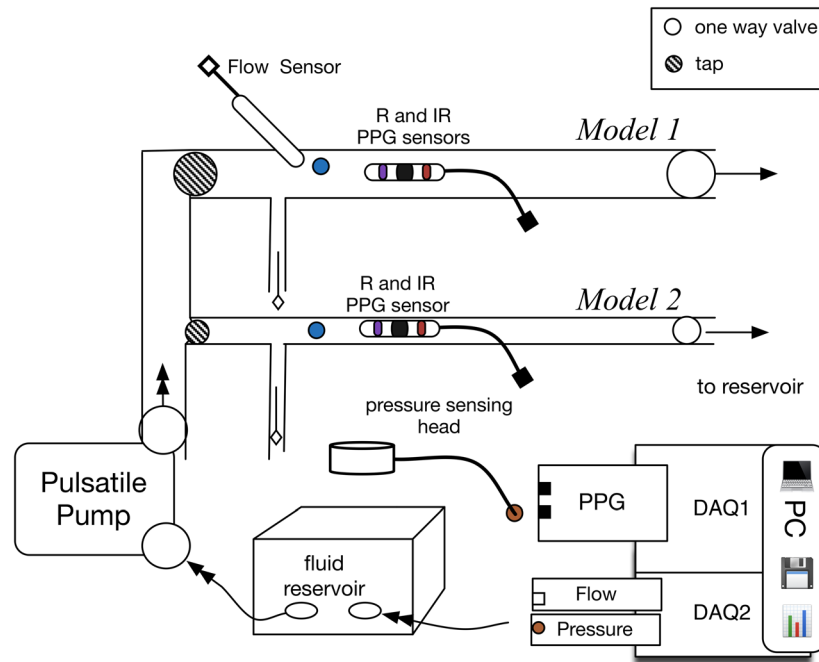


**Figure 1.** Schematic of the *in vitro* controlled setup showing arterial model, allocated sensors and processing systems.

**Table 1.** Parameters used during the experiment.

Artery properties	Model 1	Model 2
Inside diameter mm	16	6
Outside diameter mm	1.5	1
Elastic modulus (MPa)	28	17
Stroke volume (ml)	30 and 70	30 and 70
Density (g ml)	1.0914	1.0914
Pulsating frequency (Hz)	0.67, 1, 1.8	0.67, 1, 1.8

generated the digital switching clock so that the photodetector captured both wavelengths at a frequency of 900 Hz. The mixed PPG signals were fed into the demultiplexer and were then split into their respective red and infrared PPG signals. Pressure signals were digitised using the 9172-c Data-Acquisition card (DAQ2) (National Instruments, UK). R and IR PPG signals were digitised using the PCIe-6321 (DAQ1) (National Instruments, UK). All signals were digitised at a sampling rate of one kHz. Figure 2 shows the *in vitro* setup with the sensors and system configuration.

**2.2.3. Measurement protocol.** Two litres of hexahydrate cobalt nitrates ( $\text{Co}(\text{NO}_3)_2 \cdot 6\text{H}_2\text{O}$ ) in saline solution (concentration = 0.6 M) were prepared. The fluid optical spectrum was obtained using a sample of the solution in the visible and near infrared range using a spectrometer analyser (Lambda 1050, PerkinElmer, US). The reservoir was filled, and the fluid was circulated in both models simultaneously for 10 min before data collection in order to allow the system to stabilise and eliminate any bubbles. Data collection started for Model 1 for one

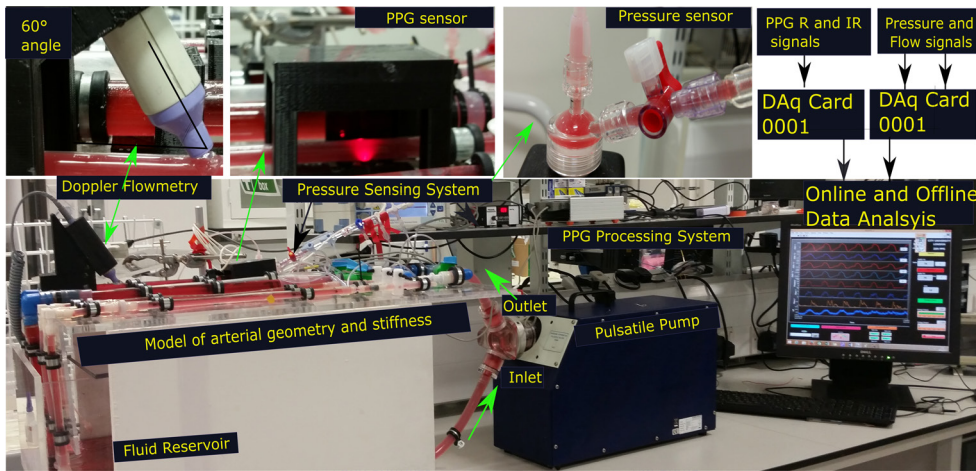


**Figure 2.** Snapshot of the developed setup showing the arterial network model, the pump, sensors configuration, processing system and data acquisition system.

minute at each pumping frequency (0.67 Hz, 1 Hz, and 1.8 Hz) at a stroke volume of 30 ml. Stroke volume was increased to 70 ml and data recording continued for one minute at the three pumping frequency set-points. The protocol was repeated for Model 2. Further parameters are listed in table 1.

**2.2.4. Data and statistical analysis.** The recorded signals were analysed in a customised Matlab script (Mathworks, US).  $PPG_{AC}$  was extracted using a band-pass filter with a cut-off frequency in the range (0.15–30 Hz).  $PPG_{DC}$  levels were obtained using a low-pass filter at a cut-off frequency of 0.05 Hz. AC magnitudes, DC levels, systolic and diastolic pressures values were obtained. Cycle-to-cycle data were tabulated for each measurement trial (frequency, stroke volume, model). Linear regression fittings were performed following the exponential  $P$ - $V$  assumed model, providing root mean square error (RMSE) and  $R$ -square ( $r^2$ ) values which indicate the goodness of curve fitting. Comparison of correlation coefficients was stated as a  $z$ -value, obtained via the Fisher  $r$ -to- $z$  transformation. Comparisons between pulsatile volume estimation methods to indirectly measure systolic pressure were assessed using Bland-Altman. The test provides the reproducibility coefficient and % of mean values (RPC (%)) and the coefficient of variation (CV); SD of mean values in %.

### 3. Results

The collected signals were of high quality. Figure 3 presents a sample of the processed signals from Model 1 at a stroke volume of 70 ml for 70 s at each pumping frequencies. Panel (a) shows the  $PPG_{AC}$  signals at R and IR wavelengths. Panel (b) shows the  $PPG_{DC}$  levels at R and IR wavelengths. Pressure signals are presented in panel (c). Forward (F1) and reflected (F2) flow velocities are presented in panel (d).

An optical spectrum of the circulating fluid was obtained from a sample as can be seen in figure 4.

Typical scattergrams and curve fits for pressure versus  $PPG_{AC}$  for both models are presented in figures 5(a) and (b) show natural logarithmic systolic pressure ( $\ln(P_s)$ ) versus R and IR  $PPG_{AC}$  for Model 1, respectively, where (c) and (d) show  $\ln(P_s)$  versus R and IR  $PPG_{AC}$

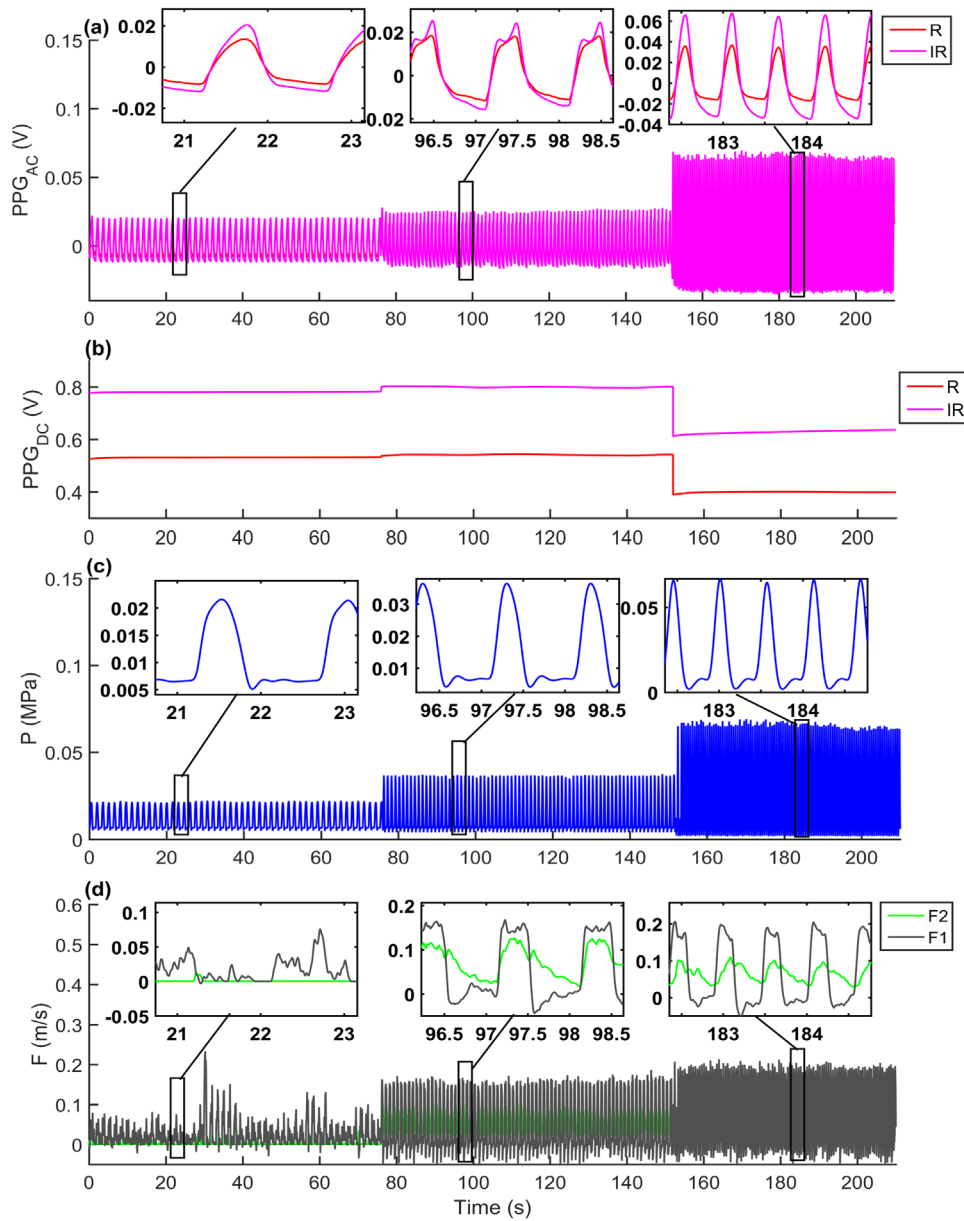


**Figure 3.** The collected signals from Model 1 at a stroke volume of 70 ml at varying pumping frequencies (0.67, 1 and 1.8 Hz). Panel (a) Red (R) and Infrared (IR) PPG<sub>AC</sub> signals, panel (b) R and IR PPG<sub>DC</sub> levels, panel (c) pressure signals and panel (d) forward (F1) and backward (F2) flow velocities

for Model 2. Points include cycle-to-cycle data of 60s at each pumping frequency and both stroke volumes. Fitting equations, values of the goodness of fit ( $r^2$  and RMSE) are also listed for each function.

Typical scattergram applying (10)–(12) demonstrating APV, NPV<sub>IR</sub>, and NPV<sub>R</sub> for Model 1 are shown in figure 6, and those for Model 2 are presented in figure 7. Points include cycle-to-cycle

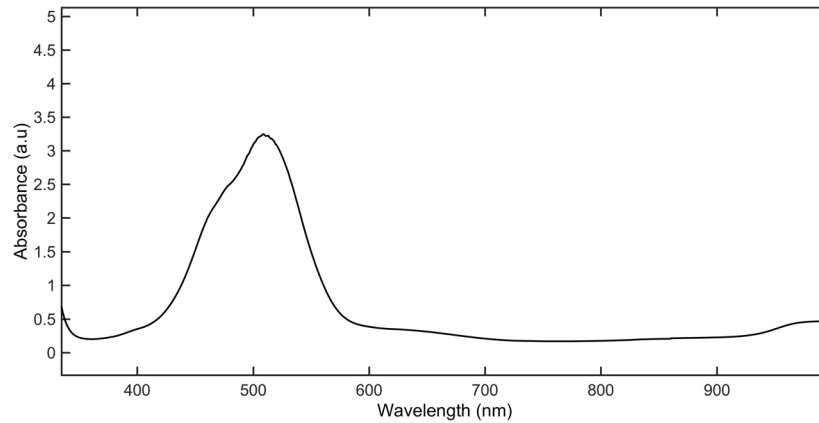


**Figure 4.** Absorption spectra for cobalt nitrate solution obtained from the spectrometer in the visible and near infrared range.

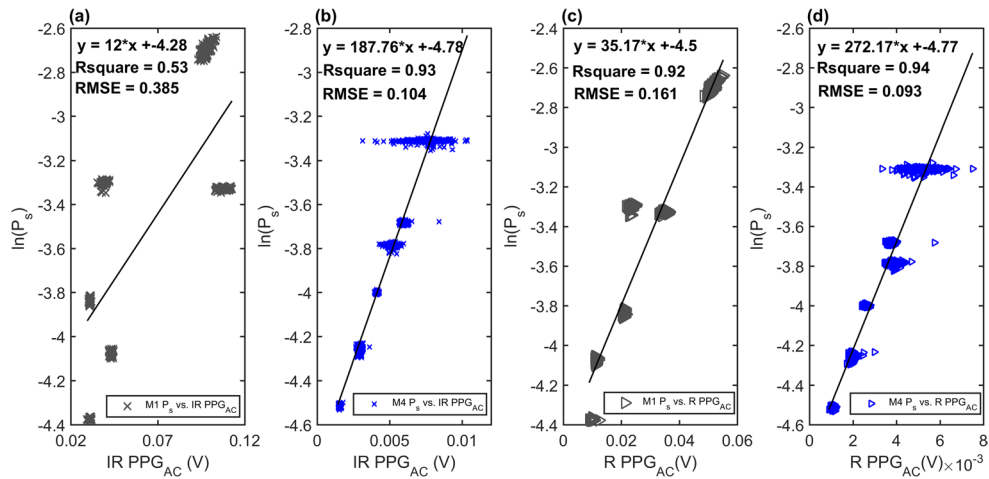


**Figure 5.** Linear fitting for natural logarithmic systolic pressure ( $\ln(P_s)$ ) versus PPGAC amplitude. (a)  $\ln(P_s)$  versus infrared (IR) PPG<sub>AC</sub> obtained from Model 1 (M1). (b)  $\ln(P_s)$  versus IR PPG<sub>AC</sub> amplitudes obtained from Model 2 (M2). (c)  $\ln(P_s)$  versus red (R) PPG<sub>AC</sub> amplitudes obtained from M1 and (d)  $\ln(P_s)$  versus red (R) PPG<sub>AC</sub> amplitudes obtained from M2. Points include cycle-to-cycle data of 60 s at each pumping frequency and both stroke volumes.

data of 60 s at each pumping frequency and both stroke volumes. Panel (a) presents  $\ln(P_s)$ -APV function. Panel (b)  $\ln(P_s)$ -NPV<sub>IR</sub> function and panel (c)  $\ln(P_s)$ -NPV<sub>R</sub>. Fitting equations, values of the goodness of fit ( $r^2$  and RMSE) are also listed for each function.

To give a representation of the range of the APV method, and to assess the agreement between  $P_s$  as measured from the pressure transducer directly and as measured from the APV, NPV<sub>R</sub>, NPV<sub>IR</sub>, R<sub>AC</sub> and IR<sub>AC</sub> methods, Bland–Altman plots (Bland and Altman 1986) are presented in figure 8 showing comparisons between the direct systolic pressure measurement method ( $P_s$ ) and  $P_s$  as obtained from the PPG estimation for all measurement methods (APV, NPV<sub>IR</sub>, NPV<sub>R</sub>, R PPG<sub>AC</sub> and IR PPG<sub>AC</sub>) for Model 1 in panels ((a)–(e)) respectively, and for Model 2 in panels ((f)–(j)) respectively.

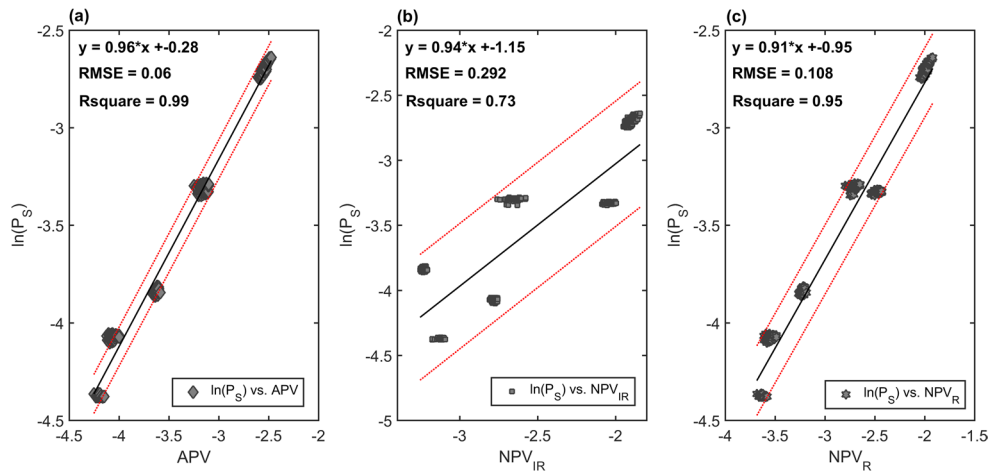


**Figure 6.** Scattergrams for  $\ln(P_s)$ -V function for Model 1. Panel (a) V is estimated using (APV). Panel (b) V is estimated using ( $NPV_{IR}$ ). Panel (c) V is estimated using ( $NPV_R$ ). Points include cycle-to-cycle data of 60 s at each pumping frequency and both stroke volumes.

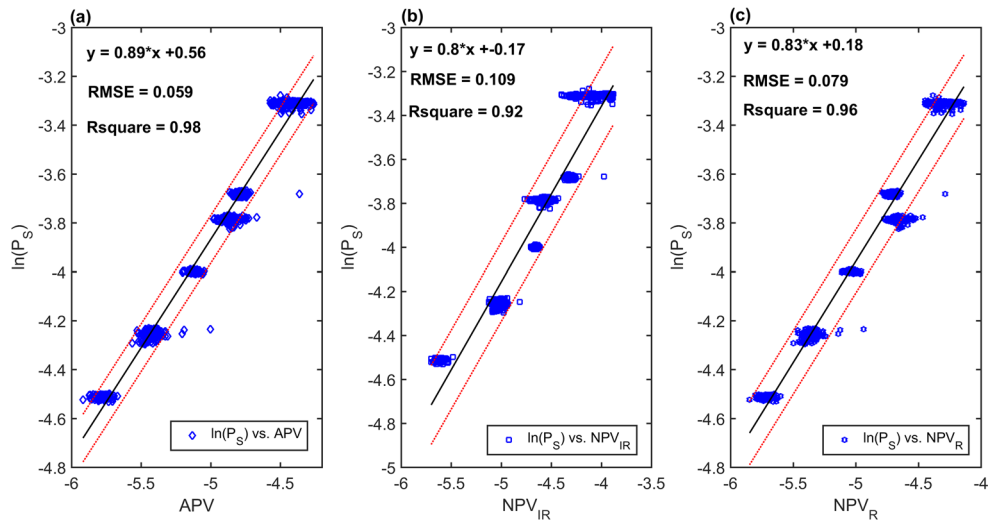


**Figure 7.** Scattergrams for  $\ln(P_s)$ -V function for Model 2. Panel (a) V is estimated using (APV). Panel (b) V is estimated using ( $NPV_{IR}$ ). Panel (c) V is estimated ( $NPV_R$ ). Points include cycle-to-cycle data of 60 s at each pumping frequency and both stroke volumes.

#### 4. Discussion

APV was advocated in the present study as a more valid measure than NPV and raw  $PPG_{AC}$  for the assessment of fluid pulsatile volume, based on the optical model expressed by Beer-Lambert's law. APV superiority to NPV and AC amplitudes are examined from a theoretical and an experimental perspective.

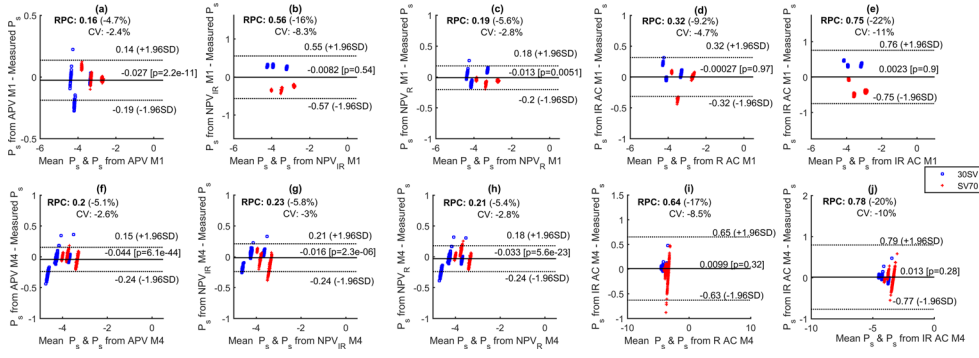


**Figure 8.** Bland–Altman plots for comparison between the direct systolic pressure measurement method ( $P_s$ ) and  $P_s$  as obtained from the PPG estimation for all measurement methods (APV, NPV<sub>IR</sub>, NPV<sub>R</sub>, R PPG<sub>AC</sub> and IR PPG<sub>AC</sub>) for Model 1 in panels (a)–(e) respectively, and for Model 2 in panels (f)–(j) respectively.

#### 4.1. Theoretical perspective

What NPV and APV denote hemodynamically can be more clearly identified when compared with AC amplitudes. NPV and APV are in direct proportion to the oscillatory component of fluid volume  $V_o$  insofar as the mean absorption coefficient and the mean concentration of the fluid do not change within the model. The pulsatile flow consists of an oscillatory and a steady component, therefore, NPV and APV taking into account both PPG<sub>AC</sub> and PPG<sub>DC</sub> components can be processed as if they are absolute values considering flow velocity profiles, and are in direct proportion to  $V_o$ . PPG<sub>AC</sub> amplitude, on the contrary, cannot be processed in such a manner and can only be measured in volts. Moreover, APV brings the advantage of considering the depth of penetration of different wavelengths. Previous studies have confirmed that IR signals penetrate deeper into tissues, which would suggest satisfactory measurement of the steady flow (Stolik *et al* 2000). However, due to the different absorption characteristics of the steady flow region, this might contribute to an error in the PPG<sub>AC</sub> signal obtained at higher wavelengths. The R PPG signal is known to reach a shallower layer, and on that ground, it can be used for a better representation of oscillatory flow. Hence, APV provides a more accurate measure of the pulsatile volume by considering oscillatory and steady flow components using the relevant wavelengths.

#### 4.2. Experimental perspective

The theoretical expectation that the directly proportional relationship between  $V_o$  holds more accurately for APV, than NPV and for both methods more than PPG<sub>AC</sub> amplitudes was indirectly supported by comparing the correlations between APV, NPV and PPG<sub>AC</sub> amplitudes with systolic pressure values using the  $P$ – $V$  exponential model. Initially, the optical spectrum of the circulating dye is seen in figure 4, which demonstrates lower absorption values in the IR region when compared to the red region. The closeness of fit is shown in figures 6 and 7 confirms the validity of the descriptive model function in the *in vitro* model. The APV correlation was highly significant ( $r^2 = 0.99$ , RMSE = 0.002,  $n = 460$ ,  $p < 0.0001$ ) for Model 1 and ( $r^2 = 0.98$ , RMSE = 0.059,  $n = 460$ ,  $p < 0.0001$ ) for Model 2. NPV obtained insufficient correlations ( $r^2 = 0.73$ , RMSE = 0.292,  $n = 460$ ,  $p < 0.0001$ ) for NPVR and significant

correlation ( $r^2 = 0.95$ ,  $\text{RMSE} = 0.108$ ,  $n = 460$ ,  $p < 0.0001$ ) for NPVIR in Model 1. In Model 2, NPV obtained significant values ( $r^2 = 0.96$ ,  $\text{RMSE} = 0.079$ ,  $n = 500$ ,  $p < 0.0001$ ) for NPVR and ( $r^2 = 0.92$ ,  $\text{RMSE} = 0.109$ ,  $n = 500$ ,  $p < 0.0001$ ) for NPVIR. In fact, correlation comparisons showed that the APV fit was significantly better than that obtained from NPVR ( $z = 12.26$ ,  $p < 0.0001$ ) and NPVIR ( $z = 25.85$ ,  $p < 0.0001$ ) in Model 1 and as obtained from NPVR ( $z = 5.54$ ,  $p < 0.0001$ ) and NPVIR ( $z = 11.17$ ,  $p < 0.0001$ ) in Model 2.

Fittings from the previously assumed hypothesis, where raw AC amplitudes are representative of the pulsatile volume are presented in figure 5. Generally, significant correlations are observed in both models from R and IR PPGAC signals. However, the Bland–Altman agreement test (figure 8) confirms, as seen in panels (d) and (e) for Model 1 and panels (i) and (j) for Model 2 that this agreement is not significant ( $p > 0.05$ ). Additionally, NPVR showed a significant agreement in both models, yet NPVIR was in significant agreement only in Model 2. This highlights that the APV method might be more beneficial in larger arteries, wherein smaller arteries, both signals penetrate deep enough to provide a good estimation of the oscillatory and steady components, hence, the NPV and APV methods provide significant agreements as observed in Model 2. Nevertheless, APV provided the strongest agreement in both models compared to the rest of the methods as seen from  $r^2$  correlation values in figures 6 and 7 and as confirmed by the Bland–Altman method comparison test and the obtained RPC and CV values seen in figure 8.

It is evident that AC amplitudes are affected by flow dynamics, whether it is pumping frequencies, stroke volumes, or a change in cross-sectional areas. The results confirm that AC amplitudes are sensitive to a change in the total section area/volume of the model and can indicate vasoconstriction or reduced blood volume, as R and IR PPG<sub>AC</sub> values were significantly less in Model 2 when compared to Model 1. Moreover, the general trend underlines that raw AC amplitudes respond to an increase in pressure values by increasing due to an increase in frequencies as seen in figure 3, however, there are cases where AC failed to reflect an increase in pressure, specifically at increased stroke volumes. By observing the DC levels seen in figure 3, we infer that PPG<sub>AC</sub> behaviour is attributed to flow profiles, where steady and oscillatory components interact to maximise the velocity of the steady layer in the centre of the tube. At the case where flow velocities increased significantly at high stroke volume in Model 1, the flow might act in a way to compensate its oscillatory component to maintain the efficiency of the steady layer. This further highlights the suitability of the APV method when compared to PPG<sub>AC</sub> amplitudes and NPV methods due to its consideration of the depth of light penetration, and dismissing potential errors in the case of steady layer expansion.

#### 4.3. Limitations of the study

This *in vitro* controlled study is aimed to address some fundamental questions, and hence, it encounters some limitations that can be addressed. The basic assumption for the derivation equations considers the fluid as a non-scattering homogeneous medium. However, this presumption is not valid for blood suspension because the light interaction through the suspension is caused by absorption, as well as scattering events (Friebel *et al* 2006). Nonetheless, the evidence is accumulating that Beer–Lambert’s law can be extended to a light scattering system (Kocsis *et al* 2006). It is also possible that light scattering of blood suspensions is constant under normal circulatory states.

The factors which can violate the directly proportional relationship between  $V_o$  were not investigated experimentally in this study ( $c$  and  $\epsilon$ ). Yet, during an *in vivo* setup,  $\epsilon$  is constant within and between subjects due to the fixed absorption coefficients of oxy and

deoxyhemoglobin at the specific wavelength. In respect to  $c$ , haematocrit changes are expected to be only a few percent due to changes in neurohormonal factors. Moreover, such changes might be indirectly represented in the obtained optical signal due to their effect on the optical density of the medium and the resultant haemodynamic changes associated with such factors.

Another limitation of this study is the use of the arbitrary values generated from the curve fitting. In fact, previous studies have considered the constant ( $n$ ) in (1) as a measure of stiffness index. It is evident that this constant indicates the increase in stiffness in Model 1 (0.96) when compared to Model 2 (0.86) (Tanaka *et al* 2011). This limitation can be overcome by introducing a calibration assessment where  $n$  and  $b$  are estimated for each subject prior to the measurement.

Finally, previous investigations of the relationship between pressure and  $PPG_{AC}$  in human studies reported the inverse of the relationship observed in this study as seen in figure 3 (i.e. light attenuation and a drop in AC amplitudes were observed with increasing pressures) (Weiss *et al* 2014). This can be attributed to the augmentation in vascular resistance with increasing pressure by the effect of vasoconstriction due to endothelial activation and, therefore, the expected drop in total volume. Hence, it is expected that the proposed approach would still be valid in a human study.

## 5. Conclusion

Despite the limitations, our study validated the proposed APV method in a large and small artery models within a wide range of mean pressure values 45–180 mmHg (0.006–0.024 MPa), controlled by means of flow rates and stroke volumes. Correlation and Bland–Altman comparisons between  $PPG_{AC}$ , NPV and APV showed that the APV fit was significantly better than that obtained from  $NPV_R$ ,  $NPV_{IR}$ , and raw R and IR  $PPG_{AC}$  amplitudes in both models. In conclusion, APV could be a potential method used in noninvasive measurement devices of blood pressure. Further, *in vivo* investigations are required to validate this method for clinical use.

## References

- Abay T Y and Kyriacou P A 2015 Reflectance photoplethysmography as noninvasive monitoring of tissue blood perfusion *IEEE Trans. Biomed. Eng.* **62** 2187–95
- Ahlstrom C, Johansson A, Uhlén F, Länne T and Ask P 2005 Noninvasive investigation of blood pressure changes using the pulse wave transit time: a novel approach in the monitoring of hemodialysis patients *J. Artif. Organs* **8** 192–7
- Allen J 2007 Photoplethysmography and its application in clinical physiological measurement *Physiol. Meas.* **28** R1–39
- Baker P D, Westenskow D R and Kück K 1997 Theoretical analysis of non-invasive oscillometric maximum amplitude algorithm for estimating mean blood pressure *Med. Biol. Eng. Comput.* **35** 271–8
- Beckett N S *et al* 2008 Treatment of hypertension in patients 80 years of age or older *New Engl. J. Med.* **358** 1887–98
- Bland J M and Altman D G 1986 Statistical methods for assessing agreement between two methods of clinical measurement *Lancet* **1** 307–10
- Burkhoff D, Mirsky I and Suga H 2005 Assessment of systolic and diastolic ventricular properties via pressure-volume analysis: a guide for clinical, translational, and basic researchers *Am. J. Physiol. Heart Circ. Physiol.* **289** H501–12
- Campbell N R, Chockalingam A, Fodor J G and McKay D W 1990 Accurate, reproducible measurement of blood pressure *Can. Med. Assoc. J.* **143** 19–24
- Chua C P and Heneghan C 2006 Continuous blood pressure monitoring using ECG and finger photoplethysmogram *Conf. Proc. Annual Int. Conf. Engineering in Medicine and Biology Society* vol 1 pp 5117–20

- Chua E C-P, Redmond S J, McDarby G and Heneghan C 2010 Towards using photo-plethysmogram amplitude to measure blood pressure during sleep *Ann. Biomed. Eng.* **38** 945–54
- de Trafford J and Lafferty K 1984 What does photoplethysmography measure? *Med. Biol. Eng. Comput.* **22** 479–80
- Foo J Y A and Lim C S 2006 Pulse transit time as an indirect marker for variations in cardiovascular related reactivity *Technol. Health Care Off. J. Eur. Soc. Eng. Med.* **14** 97–108 (PMID: 16720953)
- Friebel M, Roggan A, Müller G and Meinke M 2006 Determination of optical properties of human blood in the spectral range 250–1100 nm using Monte Carlo simulations with hematocrit-dependent effective scattering phase functions *J. Biomed. Opt.* **11** 34021
- Gesche H, Grosskurth D, Kuchler G and Patzak A 2012 Continuous blood pressure measurement by using the pulse transit time: comparison to a cuff-based method *Eur. J. Appl. Physiol.* **112** 309–15
- Gibbs N M, Larach D R and Derr J A 1991 The accuracy of finapres noninvasive mean arterial pressure measurements in anesthetized patients *Anesthesiology* **74** 647–52
- Ilies C, Bauer M, Berg P, Rosenberg J, Hedderich J, Bein B, Hinz J and Hanss R 2012 Investigation of the agreement of a continuous non-invasive arterial pressure device in comparison with invasive radial artery measurement *Br. J. Anaesth.* **108** 202–10
- James P A *et al* 2014 Evidence-based guideline for the management of high blood pressure in adults: report from the panel members appointed to the eighth joint national committee (jnc 8) *JAMA* **311** 507–20
- Jelezov C, Krajinovic L, Münster T, Birkholz T, Fried R, Schüttler J and Fechner J 2010 Precision and accuracy of a new device (CNAP™) for continuous non-invasive arterial pressure monitoring: assessment during general anaesthesia *Br. J. Anaesth.* **105** 264–72
- Jespersen L T and Pedersen O L 1986 The quantitative aspect of photoplethysmography revised *Heart Vessels* **2** 186–90
- Kocsis L, Herman P and Eke A 2006 The modified Beer–Lambert law revisited *Phys. Med. Biol.* **51** N91–8
- Kyriacou P A 2013 Direct pulse oximetry within the esophagus, on the surface of abdominal viscera, and on free flaps *Anesth. Analg.* **117** 824–33
- Members A F *et al* 2013 ESH/ESC guidelines for the management of arterial hypertension *Eur. Heart J.* **34** 2159–19
- National High Blood Pressure Education Program 2004 *The Seventh Report of the Joint National Committee on Prevention, Detection, Evaluation, and Treatment of High Blood Pressure* (Bethesda, MD: National Heart, Lung, and Blood Institute) (PMID: 20821851)
- Nijboer J A, Dorlas J C and Mahieu H F 1981 Photoelectric plethysmography—some fundamental aspects of the reflection and transmission method *Clin. Phys. Physiol. Meas.* **2** 205–15
- Payne R A, Symeonides C N, Webb D J and Maxwell S R J 2006 Pulse transit time measured from the ECG: an unreliable marker of beat-to-beat blood pressure *J. Appl. Physiol.* **100** 136–41
- Shelley K H 2007 Photoplethysmography: beyond the calculation of arterial oxygen saturation and heart rate *Anesth. Analg.* **105** S31–6
- Staessen J A *et al* 1997 Randomised double-blind comparison of placebo and active treatment for older patients with isolated systolic hypertension *Lancet* **350** 757–64
- Stokes D N, Clutton-Brock T, Patil C, Thompson J M and Hutton P 1991 Comparison of invasive and non-invasive measurement of continuous arterial pressure using the finapres *Br. J. Anaesth.* **67** 26–35
- Stolik S, Delgado J, Pérez A and Anasagasti L 2000 Measurement of the penetration depths of red and near infrared light in human ‘*ex vivo*’ tissues *J. Photochem. Photobiol. B* **57** 90–3
- Tanaka G, Yamakoshi K, Sawada Y, Matsumura K, Maeda K, Kato Y, Horiguchi M and Ohguro H 2011 A novel photoplethysmography technique to derive normalized arterial stiffness as a blood pressure independent measure in the finger vascular bed *Physiol. Meas.* **32** 1869
- Weiss E, Gayat E, Dumans-Nizard V, Le Guen M and Fischler M 2014 Use of the Nexfin™ device to detect acute arterial pressure variations during anaesthesia induction *Br. J. Anaesth.* **113** 52–60
- Yamashina A, Tomiyama H, Takeda K, Tsuda H, Arai T, Hirose K, Koji Y, Hori S and Yamamoto Y 2002 Validity, reproducibility, and clinical significance of noninvasive brachial–ankle pulse wave velocity measurement *Hypertens. Res.* **25** 359–64
- Young C C, Mark J B, White W, DeBree A, Vender J S and Fleming A 1995 Clinical evaluation of continuous noninvasive blood pressure monitoring: accuracy and tracking capabilities *J. Clin. Monit.* **11** 245–52